Pressure dependent reactions for atmospheric and combustion models†

David M. Golden

Received 13th February 2008
First published as an Advance Article on the web 26th February 2008
DOI: 10.1039/b704259k

In order to characterize reactions as functions of temperature, pressure (molecular density) and the nature of the species that constitute that molecular density, master equation solutions are required. In this *tutorial review*, the application of the Multiwell suite of codes to some reactions of interest in atmospheric and combustion chemistry is discussed, with attention given to the details of the molecular and energy transfer values. Uncertainties in data and in structural and energetic molecular parameters combine to assure the need for optimization and collaborative processing [1,2] of the entire data base when modeling practical systems.

Introduction

Many, if not most, of what are known as elementary chemical reactions are not only temperature dependent, but depend also on pressure (molecular density) and the nature of the species that comprise this molecular density. The simplest of these reactions are those that are unimolecular at high pressures, and their reverse. Examples include:

$$CH_4 \leftrightarrow CH_3 + H$$

$$Cl + NO_2 \leftrightarrow ClNO_2 \text{ and } ClONO$$

Both of these reactions involve bond dissociation on one side and radical combination in the other direction. The methane reaction is of more general interest in understanding hydrocarbon combustion and the reaction of chlorine atoms with nitrogen dioxide plays a role in parts of the atmosphere. In most pressure and temperature regimes of practical interest, besides temperature dependence, they will be pressure and bath gas dependent.

Many reactions that appear to be simple bimolecular reactions can also be dependent on pressure and the nature of the species that make up this pressure. These reactions may proceed *via* bound intermediates, which in turn may or may not be stabilized by bath gas collisions. For example, the reaction which leads to C_2 and larger hydrocarbons during methane combustion; $CH_3 + CH_3 \leftrightarrow C_2H_5 + H$ proceeds *via* an ethane intermediate. At high pressures and low temperatures, C_2H_6 is the product, but when the temperature is high enough and the pressure low enough that the ethane is not stabilized, the above products are formed.

The reaction most responsible for heat release in flames is $HO + CO \leftrightarrow H + CO_2$. This reaction proceeds *via* the HOCO radical, which is the species that is obtained by removing the non-acidic hydrogen from formic acid (**H**C(O)OH). This reaction is also very important in the atmosphere.

The reaction $HO_2 + NO \leftrightarrow HO + NO_2$ is important in the path to ozone formation in the "clean" troposphere. This reaction proceeds *via* an HOONO intermediate, which can also be a product of the reaction of $OH + NO_2$, which produces $HONO_2$ (nitric acid) for the most part.

In order to fully characterize these types of reactions, the formalism must take into account the situation wherein the time scales for chemical reaction of a particular excited species and for collisional energy transfer from that species are similar.

Under these conditions, both processes must be included in modeling experimental data, and master equations accomplish that purpose. It is not the purpose of this Review to discuss details of the master equation. The reactions discussed herein all occur along barrierless potential energy surfaces and the methods for dealing with the RRKM formulation of the rate constants is the principal focus. The hope is that sufficient molecular data and understanding exist, so that not only are laboratory data fit, but that they may be extrapolated to other regions of pressure and temperature space. For some species, theoretical methods have produced the needed molecular data,

Department of Mechanical Engineering, Stanford University, Stanford, CA 94305, USA
† One of a collection of reviews on the theme of gas kinetics.

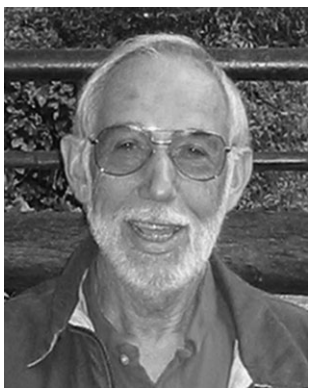

David M. Golden obtained a BS degree in chemistry from Cornell University (1956) and a PhD in Physical Chemistry from the University of Minnesota (1960). In 1961–1963 he worked at the Ballistic Research Laboratory. He then worked at SRI International, where he served as Chemistry Laboratory Director, Vice-President for Physical Science and Sr. Vice-President for Science. In 1998 he became a Consulting Professor at Stanford University. His research interests center on chemical kinetics applied to practical problems, with respect to the atmosphere and combustion. He was Editor of The International Journal of Chemical Kinetics from 1983 to 1997. In 1990 he received the American Chemical Society's Award for Creative Advances in Environmental Science and Technology.

in other cases what might be termed experience-based estimates are the best resort.

It has been the practice to codify the results of master equation calculations using variations of semi-empirical expressions. For the atmosphere these take the forms used in the IUPAC[3] and NASA/JPL[4] compilations. (These compilations are also the source of much of the data referred to in this Review. Readers are referred to them and the many references therein.)

For the NASA/JPL Evaluation[4], values of k_0, n, k_∞, and m were chosen to best describe the data according to:

$$k(M,T) = \left(\frac{k_0(T)[M]}{1+(k_0(T)[M]/k_\infty(T))}\right) 0.6^{\{1+[\log(k_0(T)[M]/k_\infty(T))]^2\}^{-1}}$$

With the rate constants represented as $k_0(T) = k_0(300\ \mathrm{K})(T/300)^{-n}$ and $k_\infty(T) = k_\infty(300\ \mathrm{K})(T/300)^{-m}$.

The IUPAC Evaluation[3] uses a somewhat different version of the equation.

$$k(M,T) = \left(\frac{k_0(T)[M]}{1+(k_0(T)[M]/k_\infty(T))}\right) \times F_c^{\{1+[\log(k_0(T)[M]/k_\infty(T))/(0.75-1.27\log(F_c))]^2\}^{-1}}$$

Both the evaluations usually describe extant data adequately. They can and do disagree when extrapolated out of the measured data range.

In modeling combustion processes it is also the practice to use the semi-empirical expressions with temperature dependence being included in the broadening factor (F_c).

Data and evaluations of same for combustion are found in Baulch *et al.*[5] to which readers are directed for many references therein.

In this Review examples are presented of several reactions such as discussed above. In large part this Review is a follow-on from the 2003 review of Barker and Golden[6] and the reader is directed to that publication and the references therein. It will become apparent that the weakness in the understanding of energy transfer and perhaps effects due to angular momentum conservation and anharmonicity, place a limit on how well data may be reproduced. This in turn emphasizes the need for optimization[7] and data collaboration tools[1,2,8]. This is an important point, uncertainties abound and statistical methods to minimize errors and evaluate experiments when developing models of practical systems, are required.

Master equation methods employed

In order to implement the master equation model, parameters must be assigned for dissociation reactions, isomerization reactions and for energy transfer. The numerous parameters are assigned by using conventional unimolecular reaction rate theory, electronic structure calculations, and ancillary thermochemical and chemical kinetics data from the literature. The master equation methods employed herein are those favored by the author for evaluating rate parameters as inputs to models of practical systems. Examples of discussions of other methods and points of view can be found in the literature.[9,10] Accuracy of all methods is limited by lack of detailed understanding of collisional energy transfer.

Rate constant expressions

In studies discussed herein, the MultiWell software package[11,12] was used for all of the calculations. The theoretical basis for this stochastic-based solution of the master equation using MultiWell is described by Barker in some detail[11] as well as in the User Manual available at the web site. In principle, each of the rate constants for dissociation and isomerization depends on vibrational energy, angular momentum and energy transfer. In the examples discussed in this Review, a one-dimensional (vibrational energy) master equation treatment is employed with centrifugal corrections for angular momentum conservation. The centrifugal corrections are made using the pseudo-diatomic approximation and by assuming the energy in the "K-rotor" (conserved rotational degree of freedom) is limited only by the total active energy and mixes freely with energy that resides in the other active degrees of freedom. These approximations are thought to be accurate and are commonplace.

RRKM theory. Unimolecular reaction rates are usually calculated using Rice–Ramsperger–Kassel–Marcus (RRKM) theory, which requires calculation of the sums and densities of internal states for all of the potential wells and transition states. Electronic structure calculations can provide normal mode vibrational frequencies and moments of inertia for the wells. In many cases, inspection of the normal mode motions enable one to distinguish vibrational modes from the torsional modes, which can be treated as hindered internal rotations. The sums and densities of states can be calculated (using the DenSum program in the MultiWell suite) by "exact counts" using the Beyer–Swinehart algorithm as adapted by Stein and Rabinovitch.[13]

According to RRKM theory the energy dependent specific unimolecular rate constant $k(E)$ is given by:

$$k(E) = \left[\frac{n^\ddagger}{n}\frac{\sigma_{\mathrm{ext}}}{\sigma^\ddagger_{\mathrm{ext}}}\right]\frac{g^\ddagger_e}{g_e}\frac{1}{h}\frac{G^\ddagger(E-E_0)}{\rho(E)}$$

where $n^\ddagger$ and n are the number of optical isomers, $\sigma^\ddagger_{\mathrm{ext}}$ and σ_{ext} are the external rotation symmetry numbers, and $g^\ddagger_e$ and g_e are the electronic state degeneracies of the transition state and reactant, respectively; h is Planck's constant, the $G^\ddagger(E-E_0)$ is the sum of states of the transition state, E_0 is the reaction threshold energy, and $\rho(E)$ is the density of states of the reactant molecule. The internal energy E is measured relative to the zero point energy of the reactant molecule and the reaction threshold energy (critical energy) is the difference between the zero point energies of reactant and transition state. This equation was written by assuming that the rotational *external* symmetry numbers, electronic degeneracies, and numbers of optical isomers were *not* used in calculating the sums and densities of states. It is, however, assumed that *internal* rotor symmetry numbers are used explicitly in the sum and density calculations and hence do not appear in the equation. Note that the quantity set off in square brackets is the reaction path degeneracy. (In practice, the sums and densities involve all vibrational, internal rotational and one dimensional external rotors, while the two dimensional rotors

of both the transition state and the molecule are taken as adiabatic.)

The reaction threshold energy is corrected for centrifugal effects according to the pseudo-diatomic model, where the reaction threshold energy at a given temperature is corrected approximately for angular momentum conservation by using a threshold energy E_0^{T} given by the following expression:

$$E_0^{\mathrm{T}} = E_0 - k_{\mathrm{B}}T\left\{1 - \frac{I_{2\mathrm{D}}}{I_{2\mathrm{D}}^{\ddagger}}\right\}$$

where $I_{2\mathrm{D}}$ and $I_{2\mathrm{D}}^{\ddagger}$ are the moments of inertia for the external two-dimensional (2-D) inactive (adiabatic) rotations of the reactant and of the transition state, respectively, and k_{B} is Boltzmann's constant. The resulting expression for $k(E)$ corresponds to that given by eqn 3.31 in Holbrook, Pilling and Robertson.[14]

For a thermal distribution, recombination reaction rate constants (k_{rec}) are related to the corresponding unimolecular rate constants (k_{uni}) according to the equilibrium constant (K). Thus at the high pressure limit we have the relationship

$$K = \frac{k_{\mathrm{rec}}^{\infty}}{k_{\mathrm{uni}}^{\infty}}$$

Equilibrium constants can be calculated using the computer code Thermo in the MultiWell suite[12] which employs conventional statistical mechanics formulae for separable degrees of freedom that include harmonic and anharmonic oscillators, free and hindered internal rotors, and external rotational degrees of freedom.

In recombination reactions, the two reactants come together to form a highly excited adduct, which can re-dissociate, be collisionally deactivated, and react *via* other reaction channels. The chemical activation energy distribution[11] describes the nascent energy distribution of the complex formed in the recombination reaction:

$$y_0^{(ca,i)}(E)\mathrm{d}E = \frac{k_i(E)\rho(E)e^{-\frac{E}{k_{\mathrm{B}}T}}\mathrm{d}E}{\int_{E_0}^{\infty} k_i(E')\rho(E')e^{-\frac{E'}{k_{\mathrm{B}}T}}\mathrm{d}E'}, \quad \text{for } E \geq E_0$$

where $y_0^{(ca,i)}(E)$ is the energy distribution of molecules formed *via* reaction channel i, which has energy threshold E_0 and specific rate constant $k_i(E)$, $\rho(E)$ is the density of states in the new molecule, and the zero of energy for this equation is at the zero point energy of the newly formed species. Starting with the above distribution obviates some of the issues arising from using a thermal distribution and thus reduces difficulties associated with different time scales for energy transfer and reaction. Since Multiwell[11,12] produces error calculations, sufficient numbers of collisions can be employed to reduce error to acceptable limits.

Loose transition states. For "loose" transition states, the properties of the transition state depend sensitively on angular momentum and the detailed shape of the interaction potential. In the absence of other information, it is possible to estimate the rate constant by using variational transition state theory with a calculated potential energy surface.[15] When the high pressure rate constant is known, however, it is more convenient to use a "restricted" Gorin Model with a "hindrance parameter" selected to reproduce the known rate constant.[16]

According to this Gorin model the two molecular fragments rotate independently of one another while separated at the distance corresponding to the centrifugal maximum (r_{max}) of the effective potential of the bond being broken. For those systems with loose transition states considered herein, the rotations of both fragments and the over-all transition state are treated approximately as symmetric tops. The over-all transition state has a 2-D external adiabatic rotation with moment of inertia given by $I_{2\mathrm{D}}^{\ddagger} = \mu r_{\mathrm{max}}^2$, where μ is the reduced mass of the two fragments, and a 1-D external rotation (the "K-rotor") with moment of inertia I_k. The K-rotor is not adiabatic and is assumed, according to the usual approximation,[16] to mix energy freely with the active vibrations. The internal rotations of fragments A and B are characterized by 2-D rotations with moments of inertia I_a and I_b, respectively, and an internal rotation with reduced moment of inertia I_r. Given the uncertainties in many quantities, the K-rotor is often kept the same in both molecule and transition state.

In the restricted Gorin model[16] it is assumed that the two fragments interfere sterically with each other and thus cannot rotate freely. The effect is to reduce the available phase space and hence reduce the sum of states. Operationally, a "hindrance" parameter η is defined, which can vary from zero (free rotation) to unity (completely hindered). The 2-D moments of inertia I_a and I_b are multiplied by the factor $(1 - \eta)^{1/2}$ to obtain the effective 2-D moments of inertia used for calculating the sum of states.

In general, for many reactions of practical import, the potential function describing the breaking bond is not known, but the Lennard-Jones potential has often been chosen for its simplicity and because it has the long range dependence on r^{-6} expected for many long range potentials. It does not describe a chemical bonding interaction very well at short range (near the potential minimum energy), however. For the Lennard-Jones potential, the moment of inertia for the two-dimensional adiabatic external rotation is given by $I_{2\mathrm{D}}^{\ddagger} = \mu r_e^2(6D_e/RT)^{1/3}$, where r_e is the equilibrium bond distance, μ is the reduced mass, and $D_e = D_0 - \Delta E_z$, where D_0 is the bond dissociation enthalpy at 0 K, ΔE_z is the zero point energy difference between products and reactants, and R is the gas law constant. Use of Morse (used in many of the examples in this Review) or Varshni potentials changes some fitting parameters, but not the qualitative result.

Energy transfer. Energy transfer with the various bath gases was computed using, the often employed, exponential down probability function and the value of $\langle \Delta E_{\mathrm{d}} \rangle$. It has proven difficult to make a systematic evaluation of this quantity. There is some evidence that it should be expected to be linearly dependent on temperature, but this is not always borne out. The values ascertained by fitting data are not completely independent of other fitting parameters. There exist alternatives to the exponential down model. Barker lists thirteen such choices in the MultiWell Users Manual.[12] Many require more than one parameter and it is not clear that any are more general or that there are specific instances in which to use a given formulation.

Examples

$CH_4 \leftrightarrow CH_3 + H$

This section summarizes a study by Golden.[17] *References are found in that work*. Treatment as described above has been carried out for several reacting systems. A simple example is the methane reaction mentioned earlier. As pointed out, this reaction is important in all hydrocarbon combustion, given the abundance of both methyl radicals and hydrogen atoms under those circumstances.

Some years ago, Stewart *et al.*[18] attempted, using a RRKM psuedo-strong-collision formulation, to represent the data for the title system by fitting data for the decomposition of methane in methane itself. They also compared the result to data in the reverse direction at lower temperatures. In addition they examined the reported isotopic exchange reactions and were able to fit these.

In the GRI-Mech optimization,[7] a model for natural gas combustion, it was necessary to increase the pressure dependent rate constant computed from the parameters in Stewart *et al.*[18] Given the large number[5] of studies, experimental and theoretical, since the Stewart *et al.*[18] paper and the plans of the PrIMe project[8] to use capabilities of cyberinfrastructure to create a more up-to-date mechanism for natural gas combustion than GRI-Mech,[7] an evaluation of the methane system using master equation methods was undertaken. The idea is to use a consistent model for reactions of this type to produce rate constants as functions of temperature, pressure and nature of the bath gas that can be used as reasonable starting points in an optimization of a particular model of a practical system.

The analysis proceeded in the following fashion: (All other examples in this review follow a similar protocol.)

1. The structure and frequencies for CH_4 and CH_3 were taken from the literature.

2. Using these geometries, the moments of inertia of methane and methyl radical were computed. The two-dimensional (2D) moment of inertia is the root mean square of the two largest moments (J moment). The center of mass distance in methane is calculated from the J moment and the reduced mass of CH_3 and H, treated as point masses (pseudo-diatomic approximation) by dividing by the reduced mass and taking the square root. In a small deviation from Stewart *et al.*,[18] who used a Lennard-Jones potential, a Morse potential computed using this center of mass coordinate (which is greater for each molecule than the bond length of the breaking bond) and the known well depth was employed. The position of the centrifugal maximum was obtained by adding the rotational energy at the maximum, assumed[14] to be kT and setting the derivative to zero. These values were then used to replace the CH_3–H equilibrium bond length and moments of inertia were calculated for this new entity, *viz*. the transition state. This was done at each temperature of interest. A Lennard-Jones potential gives a larger value for the position of the centrifugal maximum and would have altered the moments of inertia somewhat. However this could have been easily compensated by use of a larger hindrance of the rotors in the transition state, with very little effect on the outcome.

3. Frequencies and moments of inertia for the transition states were taken to be those of the CH_3–H moiety described above and of CH_3. The two dimensional rotor of CH_3 was hindered to match the high pressure rate constant.

4. Energy transfer with the various bath gases was computed using the exponential down probability function and the value of $\langle \Delta E_d \rangle$. Normal uncertainties in this and the other collision parameters do affect the fitting of the calculated curves to the results, but often the data can be accommodated with only small changes in these quantities. As will become apparent below, the data could be fit for this CH_3 + H system by treating $\langle \Delta E_d \rangle$ in a systematic way. The parameter values are given in Table 1.

5. The key variables which determine the extent of rate constant pressure dependence are the degree of hindrance (which determines the high pressure limiting A factor) and the critical energy (which, together with the energy transfer parameter, determines the low-pressure limiting rate constant). In this case the critical energy is well-known. The choice of values of the energy transfer parameter is discussed in the next sections.

Table 1 Parameters for MultiWell calculations

CH_4		
Critical energy at 0 K/kcal mol^{-1}		103.3
Vibrational frequencies/cm^{-1}		3019(3), 2917, 1534(2), 1306(3)
(J-rotor) Adiabatic moments of inertia/AMU A^2		3.19
(K-rotor) Active external rotor/AMU A^2		3.19
Symmetry; Electronic degeneracy; Optical isomers		12; 1; 1
H–CH_3 (Gorin transition state)		
Frequencies/cm^{-1}		3184(2), 3002, 1383(2), 580
(J-rotor) Adiabatic moments of inertia /AMU A^2 300 K, 500 K, 1000 K, 1500 K, 2000 K		27.9, 24.9, 21.1, 19.0, 17.6
(K-rotor) Active external rotor/AMU A^2		3.60
Moments of inertia active 2-D rotor/ AMU A^2		1.75
Hindrance (To match k_∞/cm^3 molec^{-1} s^{-1} = 3.5 × 10^{-10}) 300 K, 500 K, 1000 K, 1500 K, 2000 K		78%, 79%, 80%, 82%, 83%
Symmetry; Electronic degeneracy; Optical isomers		3; 1; 1
Collisions: (σ/A^2; ε/K;)		
	CH_4	3.33; 94.9
	Ar	3.75; 98.3
	He	2.55; 10.0
$\langle \Delta E \rangle_{300}$/cm^{-1}		100(He), 150(Ar), 400(CH_4), 500(C_2H_6)
$\langle \Delta E \rangle_{down}$/cm^{-1} = $\langle \Delta E \rangle_{300}$/cm^{-1} × ($T$/300)		

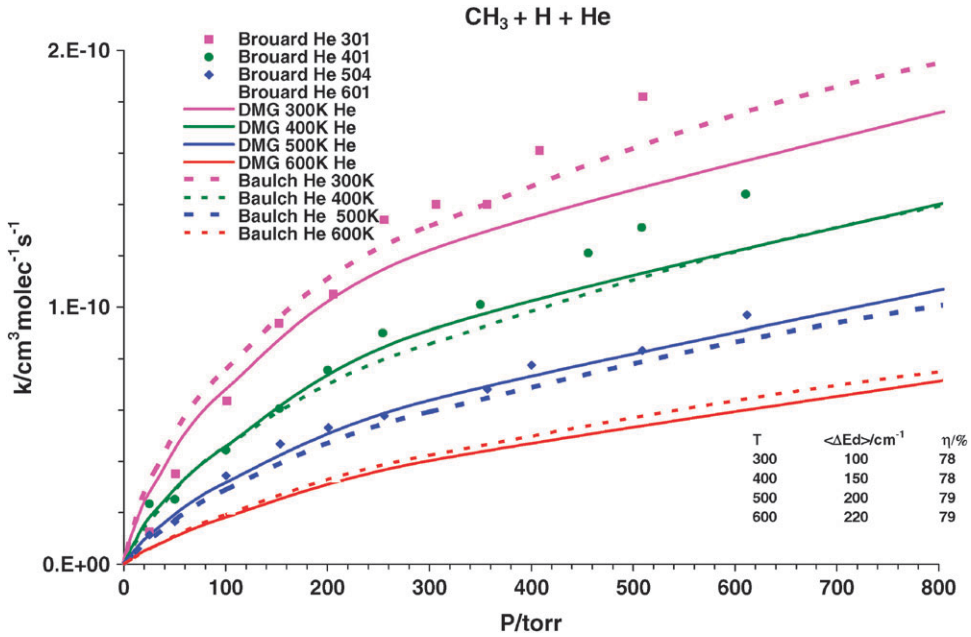

Fig. 1 Rate constants for methane formation from methyl radical combining with H-atom in the presence of He as a function of temperature and pressure. The solid lines with the appellation DMG were computed as described in the text. Those labeled Baulch are from Baulch *et al.*[5] The data may be found in Baulch *et al.*[5] The box shows values of energy transfer parameters and hindrance parameters used.

6. Since the MultiWell code[11,12] used here, as for other RRKM codes, calculates the unimolecular rate constants for dissociation, it is necessary to know the equilibrium constants in order to compute the association rate constants. The equilibrium constants were calculated using the Thermo code within MultiWell, which employs the same input information (the enthalpy change and the structure and frequencies of CH_4, CH_3 and H) as for the RRKM calculation itself.

Data in He. Rate constant values for the methane system in He were treated as described above and the results compared to data. Fig. 1 shows excellent reproduction of the Baulch[5] values as well as agreement with the data. In fact, the value of $\langle\Delta E_d\rangle$ for He at 300 K of 100 cm^{-1} is in the range of expectation. (It can also be shown that a value of the energy transfer parameter of 500 cm^{-1} for ethane as the bath gas fits the expression in Baulch *et al.*[5] for those data.)

Armed with these results, values of the dissociation rate constant in He were modeled at 1098 K, 1123 K and 1148 K by assigning $\langle\Delta E_d\rangle_T = \langle\Delta E_d\rangle_{300}(T/300)$, with $\langle\Delta E_d\rangle_{300} = 100$ cm^{-1}. Since all three of these temperatures are close to 1000 K, the value of the hindrance parameter for that temperature was used for all three temperatures. (Values of $I^{\ddagger}/I$ that are used to locate the centrifugal barriers do not change significantly in this range.) The results suggest that this procedure is adequate. A small reduction in $\langle\Delta E_d\rangle_T$ will improve the results at the lowest pressures, but the results are sparse and the recalculation doesn't seem justified. The agreement with Baulch *et al.*[5] is excellent.

Data in Ar. The original attempt to fit the Ar data and the Baulch[5] expression required very uncharacteristic values of $\langle\Delta E_d\rangle_T$. Given the rational results when examining the data in He, it was postulated, based on general experience, that if $\langle\Delta E_d\rangle_{300}$ for He was 100 cm^{-1}, than the value for Ar should be about 150 cm^{-1}.

Comparison to fits from the expressions in Baulch *et al.*[5] shows roughly a fifty percent decrease at 300 K and a factor of four increase at 2000 K. At the other temperatures the differences are no more than a factor of two. Comparison can be made with data for methane dissociation. It is no surprise that the data near 1000 K can be represented either by Baulch *et al.*[5] or by methods suggested here. Because the values essentially overlap at 1000 K. Fig. 2 illustrates the fit to data in the neighborhood of 2000 K, where differences between the values in Baulch *et al.*[5] and those used here are about a factor of four. Here the data are better fit using the modified values of $\langle\Delta E_d\rangle_T$.

Data in CH_4. Given the values of $\langle\Delta E_d\rangle_{300}$ of 100 cm^{-1} for He, 150 cm^{-1} for Ar and 500 cm^{-1} for ethane, it was postulated that the value for methane would be 400 cm^{-1}. This was then treated as above, $\langle\Delta E_d\rangle_T = \langle\Delta E_d\rangle_{300}(T/300)$. When comparison with dissociation data[5] is made the fits to the data are excellent.

$HO + NO_2 \leftrightarrow HONO_2$ (and HOONO)

This section summarizes an earlier study.[19] *References are found in that work.* This reaction, or rather these reactions, are very important in the atmosphere.

Experimental data

There is a large body of experimental data for this system. Much of it has been discussed in the literature.[19] Some newer data have been published as well.[20] An overview of this system attempting to account for HO-loss kinetics, isotopic scrambling and the formation of $HONO_2$ from HO_2 + NO, has led

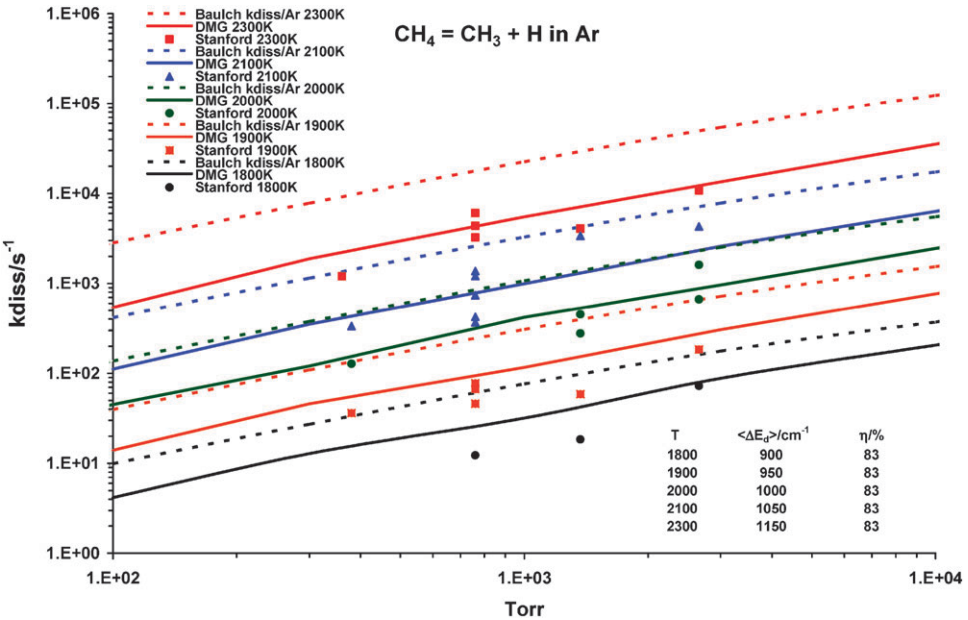

Fig. 2 Rate constants for methane dissociation in the presence of Ar in the temperature and pressure range corresponding to data near 2000 K. The solid lines are computed as those labeled DMG in Fig. 1, but with the values of $\langle \Delta E_d \rangle_T$ given in the box. The dotted lines are from Baulch *et al.*[5] (Temperature data represent a binning of values at approximately the temperature indicated.)

Zhang and Donahue[21] to propose a potential energy surface that is compatible with all the data.

Models

The potential energy surface for the HO + NO_2 system is a bit complex. The combination of an HO with an NO_2 can lead to $HONO_2$ and, according to some calculations,[19] three stable forms of HOONO. In the calculations discussed herein, the dissociation of each of the four species has been treated using MultiWell[11,12] and the resulting rate constants are multiplied by the appropriate equilibrium constant and added to obtain the total rate coefficient for the HO + NO_2 reaction. No theoretical calculations show any low energy connection between $HONO_2$ and HOONO. The fact that there are low energy connections *via* rotations around the appropriate bonds, among the HOONO isomers doesn't affect the results. Since the data to be explained are based on the combination reactions to form $HONO_2$ and HOONO, equilibrium constants for the overall processes to form these species are required. Frequencies and structures of the molecules were from calculations to be found in[19] in the same form as Table 1. Again, the transition states were treated as hindered-Gorin species and energy transfer was treated using a single exponential collision model.

Results

Data at or near 300 K and computed curves are shown in Fig. 3. These fits were all computed using modified Lennard-Jones potentials for the HO–NO_2 interaction.

Fig. 3 shows data at 300 K in both N_2 and He, along with calculated values of the rate constant as a function of pressure (molecular density) for the individual pathway to $HONO_2$ and the sum of the three paths to HOONO as well as the sum of all loss of HO and NO_2 resulting from the sum of these two quantities. It is only in the very high pressure He data that the effect of the HOONO pathway becomes apparent. The values of $\langle \Delta E_d \rangle$ of 250 cm^{-1} for He and 800 cm^{-1} for N_2 are higher than might be expected. Usually values of about 100–150 cm^{-1} for He and about 200–400 cm^{-1} for N_2 are suggested. This may be some indication that the largest uncertainty in the model for reactions of this general type concerns energy transfer. This becomes more apparent below. It is possible that significant changes in the moments of inertia of the transition states involved would yield lower values for the energy transfer parameter. At some point, given the state of knowledge, this becomes an exercise.

Although there is little doubt that the species HOONO is formed along with $HONO_2$ in the interaction of HO with NO_2, the model suggests that no more than 15–20% of HOONO is formed at 220 K and about one atmosphere. It is difficult to confirm this within the combined uncertainty of the data and the model. The data at 300 K, with He pressures of the order of 10 atmospheres or greater, clearly show some effect.

$CH_3O_2 + NO_2 \leftrightarrow CH_3O_2NO_2$

This section summarizes a previous publication.[16] *References are found in that work*. In this study the data for the system CH_3O_2 + NO_2 ↔ $CH_3O_2NO_2$ were examined. Data exist for rate coefficients for this system in both directions. The extant data sets cover a rather limited range of temperature and pressure, nevertheless the range of atmospheric interest is well-covered. Since the association process is of some atmospheric interest, the data have been evaluated by both the NASA[4] and IUPAC[3] panels. The panel values each do an adequate job of fitting all the data.

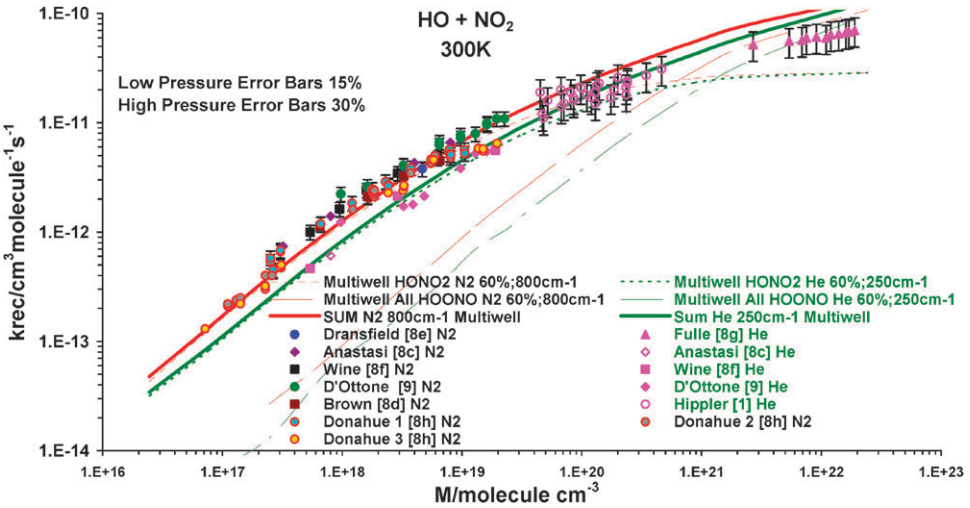

Fig. 3 Data for the rate constant for the reaction between HO and NO_2 at 300 K, from various sources, as indicated in the legend.[19] The dashed red curve is the MultiWell calculation for a 60% hindered-Gorin transition state and 800 cm^{-1} energy transfer step size in N_2 for the sum of HOONO formation due to the three isomers.[19] The dotted red curve is the MultiWell calculation for a 60% hindered-Gorin transition state and 800 cm^{-1} energy transfer step size in N_2 for $HONO_2$ formation.[19] The red solid curve is the sum of these two curves. The green curves are identical except that they are for an energy transfer step of 250 cm^{-1} in He. The pink data points are all in He. All others are in N_2.

Equilibrium constant for $CH_3O_2 + NO_2 \leftrightarrow CH_3O_2NO_2$

Using the parameters from the best fit results to the data in each direction, the equilibrium constant may be obtained. (Of course, the equilibrium constant might be obtained from the rate constant values in each direction obtained at identical temperatures and pressures.) However, there are several ways that the equilibrium constant might be extracted. Either the high pressure limits or the low pressure limits should in principle be appropriate. They, in fact give values that differ by about 50% in the temperature range where the reaction has been measured in both directions. Extrapolating between 200 K and 400 K leads to differences ranging from 0.5 to 5, illustrating the real uncertainty range.

Comparison with RRKM/ME calculations

In the standard method used in this Review, MultiWell[11,12] was used to compute the pressure dependence of k/k_∞ as a function of bath gas density. The hindered-Gorin transition states were chosen to match the Arrhenius parameters for the high-pressure rate coefficients in the decomposition direction.

Operationally(in analogy with previous cases):

1. Structure and frequencies for $CH_3O_2NO_2$ were computed at the B3LYP/6-311+G** level using Spartan.[22]

2. Using a Morse potential moments of inertia are computed as detailed above.

3. Frequencies for the transition state were the frequencies of NO_2[19] and CH_3O_2, the latter from quantum calculations, see Golden.[16]

4. Hindrance values were chosen to reproduce the statistically determined high pressure A-factor and critical energies were chosen to reproduce the activation energy for the dissociation process.

5. Energy transfer with the nitrogen bath gas was computed using the exponential down probability function and the value of $\langle \Delta E_d \rangle$ was adjusted in an attempt to reproduce the fitted curves.

6. Values were multiplied by the equilibrium constant to obtain rate coefficients in the combination direction.

The "hindered-Gorin" transition state

Transition states were chosen to match the high pressure parameters from fitting either the NASA or IUPAC formulae to the data[16] on dissociation of $CH_3O_2NO_2$. Once the values that lead to the high-pressure parameters were fixed, the value for $\langle \Delta E_d \rangle$, the energy transfer parameter in nitrogen used in the exponential down model of energy transfer, was chosen. The values for fitting the NASA expressions are 600 cm^{-1} and 400 cm^{-1} at 300 K and 223 K. There is sufficient uncertainty in these values that a temperature independent value of 400 cm^{-1} would also fit.

$CH_3 \leftrightarrow CH_2 + H$ and $CH + H_2$

This section summarizes a study by Vasudevan et al.[23] *References are found in that work.*

RRKM/ME analysis

Experimental results from Vasudevan *et al.*[23] yield the rate constants and thus the branching ratio for this system. Unlike other studies[5] they found no discernable pressure dependence to the branching ratio. Attempts were made to reproduce the experimental results with a master equation RRKM analysis. The MultiWell suite[11,12] was used for the calculations. Calculations were performed at 2800 K. The required parameters include thermochemical values for CH_3, CH_2, CH, H_2 and H. These allow the calculation of the equilibrium constants. The values obtained at 2800 K were $K(CH_2 + H \leftrightarrow CH_3)$/molecule $cm^{-3} = 2.97 \times 10^{16}$ and $K(CH + H_2 \leftrightarrow CH_3)$/molecule $cm^3 = 1.26 \times 10^{17}$. Using expressions in the

Table 2 Comparison of calculated and experimental values at 2800 K and 1 atm

	$k_{1b}(CH_2 + H)$ [$cm^3\ mol^{-1}\ s^{-1}$]	$k_{1a}(CH + H_2)$ [$cm^3\ mol^{-1}\ s^{-1}$]	$k_{1b}/(k_{1a} + k_{1b})$
Experiment	7.9×10^8	1.5×10^9	0.33
Calculated	9.8×10^8	1.8×10^9	0.39

literature for the high-pressure-limit rate constants for the reactions as written above yield for 2800 K, k^∞/molecule cm^{-3} $s^{-1} = 4.5 \times 10^{-10}$ and k^∞/molecule cm^{-3} $s^{-1} = 2.8 \times 10^{-10}$, respectively. Thus, k^∞ $s^{-1} = 1.3 \times 10^7$ and k^∞ $s^{-1} = 3.5 \times 10^7$ are the values in the dissociation direction.[23]

Values for calculation of the sums and densities of states of the transition states between CH_3 and the two channels that yield $CH_2 + H$ and $CH + H_2$ were taken to reproduce the high-pressure-rate parameters given above. The transitional modes were treated as hindered rotors in the hindered Gorin method as employed in earlier examples in this Review.

Using a Morse potential the centrifugal barriers were computed for the transition state leading to $CH_2 + H$, from the moments of inertia as earlier. For the transition state leading to $CH + H_2$, the potential is more complicated than a Morse function. The surface can be fit with a Morse potential at $CH–H_2$ distances greater than 1.33 Å. This was used as the starting point for computing the moment of inertia for that transition state. The probability for energy transfer was treated using the exponential down function.

When calculations were performed at 1 atmosphere of Ar using the best inputs determined as above, the $CH + H_2$ channel did not appear. Since this is the channel with the most complex potential energy surface, the value for the two dimensional moment of inertia in the transition state was modified until the correct branching ratio could be attained. This required a change from 11.0 to 12.89 AMU-$Å^2$. This change together with a value for ΔE_{down} of 150 cm^{-1} in the exponential down model could fit the data reasonably well. The results of a representative calculation are compared with the experimental values in Table 2. A pressure effect with a magnitude similar to that in the literature could not be discerned in either the calculation or the experiments. Note, that many parameter changes were tried (energy transfer was increased and decreased, Gorin hindrance was varied, the parameters were not required to fit the reported values of the reverse rate constant), none of which yielded a significant pressure dependent fall-off.

An observation

The pressure and temperature dependence of the reactions discussed up to this point can apparently be mimicked within reasonable uncertainty bounds by the methods employed. The next set of reactions proved to be much more recalcitrant.

$ClO + ClO \leftrightarrow Cl_2O_2$

This section summarizes a study by Golden.[24] References are found in that work. This reaction is thought to play a key role in the chemistry that creates the "Antarctic Ozone Hole". The reaction of ClO with another ClO is expected to yield ClOOCl. The rate constant is expected to be a function of temperature, pressure and nature of the bath gas. This reaction is invoked in models of Antarctic Stratospheric chemistry. The ClOOCl is thought to then be the source of Cl-atoms *via* photolysis. The ClOO fragment is thought to yield another Cl-atom rapidly. It is possible for the product to also be ClOClO. To the extent that this species is formed, the proposed chemistry would also change.

The equilibrium constant, besides being needed for the rate constant calculations, is needed in atmospheric modeling as well, in order to model the competition between photolysis and thermal dissociation of ClOOCl.

Master equation and RRKM modeling

Using the Morse parameters available in the literature and, as before, making the usual assumption that rotational energy at the maximum along the PES determined by adding rotational energy to the computed PES is given by kT,[14] the value of the interaction distance can be computed at any temperature. Using these values, the moments of inertia of the transition state may be calculated at each temperature by using the reported structures for the molecules and lengthening the O–O or O–Cl bonds respectively. Since the transition states are quite loose, once again they are treated as two independent ClO moieties restrained by some hindrance. The angles were adjusted in the moment of inertia calculation to keep the K-rotor the same value as in the molecule.

Equilibrium constant and bond dissociation energies

A value of the equilibrium constant may be obtained from combining third-law calculations based on the extant data.[4] Such an exercise using reported frequencies yields a value of $\Delta H_{f,0}(ClOOCl) = 31.7$ kcal mol^{-1}. In a direct measurement Plenge *et al.*[25] reports 32.1 ± 0.7 kcal mol^{-1}. Using a compromise value of $\Delta H^\circ_{f,0} = 31.9$ kcal mol^{-1}, yields an equilibrium constant expressed in the NASA/JPL format of: K/cm^3 $molecule^{-1} = 2.5 \times 10^{-27} \exp(8461/T)$. This corresponds to a critical energy of 16.4 kcal mol^{-1}. A study of the dissociation reaction combined with values for the combination reaction agrees with this value. (Assuming that only ClOOCl is formed from the reaction of two ClO radicals.)

Hindrance values

Hindrance values were chosen to yield rational high pressure A-factors. The data, being very close to the low pressure limit the calculations are fairly insensitive to this choice.

Energy transfer parameters

Several values were tried in order to fit the low pressure data. Since the data are much closer to the low pressure limit than to the high pressure limit and fitting is more sensitive to these values than to the ones above.

Results

Empirical fitting

The data come from three laboratories.[4] Empirical fits used in the NASA/JPL compilation do capture the data in the experimental range, which covers most of the range of atmospheric interest, but the parameters are puzzling. Parameters in the NASA format may not always fit theoretical values of rate constants and the fall-off exactly, but they usually can be rationalized with theory. For this reaction, the low pressure rate constant is sufficiently high that rationalization with theory requires essentially 100% efficiency for energy transfer, an unlikely scenario. At the same time, although the data are less sensitive to this value, the high pressure parameter has a somewhat high negative temperature dependence. Most radical-radical combination reactions have high pressure rate constants close to temperature independent or with slight negative temperature dependence.

RRKM and master equation modeling. Table 3 shows the molecular parameters used in both pseudo-strong collision RRKM and Master Equation calculations. The only difference between the two being the use of an exponential down energy transfer probability function with a choice of the average energy transferred in a down step ($\langle\Delta E_d\rangle$) in the MultiWell calculations and a value of the average overall energy transferred ($\langle\Delta E_{all}\rangle$) together with the formula relating collisional efficiency, β_c, to this quantity. ($\beta_c/(1-\beta_c^{1/2}) = -\langle\Delta E_{all}\rangle/F_E kT$, where F_E is the energy dependence of the density of states.) These calculations yield essentially the same results in the range of the data considered. In both cases, the ClOClO channel contributes about 10–15% and inordinately high energy transfer for nitrogen is required. Values of $\langle\Delta E_d\rangle$ for N_2 at 200 K of 1000 cm^{-1} and values of β_c of almost unity are required to fit the data. It has been thought possible that a "chaperone" mechanism, as opposed to the "energy transfer" model assumed in this work, governs either the energy transfer or the chemistry or both. Liu and Barker[26] use trajectory calculations on a reasonable potential energy surface to seemingly rule this out.

Fig. 4 shows the results of a calculation that includes both ClOOCl and ClOClO as products of the reaction. These species are also connected *via* an isomerization barrier. The value of $\langle\Delta E_d\rangle$ used was 400 cm^{-1}, a "normal" value for nitrogen as the bath gas.

There are some other parameters that could be changed. The hindrance in the transition states for each channel has been taken as the same as has the energy transfer parameter. In fact, one could ignore even the magnitude of the moments of inertia for the transition state that dictate the affect of conservation of angular momentum, choosing perhaps a shorter interaction distance as might have been predicted from a simple Lennard-Jones or Morse interaction. It has been suggested that perhaps the rotational degrees of freedom treated adiabatically should be included as active in the state density, but such calculations seem to make little difference. A possible failing is the lack of inclusion of anharmonicity in the density of states calculations. Also, the energy difference between ClOOCl and ClOClO might be altered. At this point changing these is just an exercise. High pressure experiments would help.

$Cl + NO_2 \leftrightarrow ClNO_2$ and ClONO

This section summarizes amore detailed study.[27] *References are found in that work*. The reaction of chlorine atoms with nitrogen dioxide has long been known[4] to yield both ClONO, presumably in both *cis* and *trans* forms, and $ClNO_2$, with the former accounting for about 80% of the yield at temperatures around room temperature and pressures up to about one atmosphere. Chang *et al.*[28] would seem to have explained

Table 3 Molecule and transition state properties

(a) ClOOCl and ClO–OCl	
ClOOCl	
Critical energy at 0 K/kcal $mole^{-1}$	16.45
Frequencies/cm^{-1}	844, 638, 551, 443, 326, 127
Product of adiabatic moments of inertia/AMU-A^2	213.2
Moment of inertia: active external rotor/AMU-A^2	38.2
ClO–OCl (Transition state)	
Frequencies/cm^{-1}	866, 866
Anharmonicities/cm^{-1}	7.5, 7.5
Active external rotor/AMU-A^2 (K-rotor)	39.1
Mean of adiabatic moments of inertia/AMU-A^2 (J-rotor) 263 K; 200 K; 183 K	1210; 1281; 1305
Hindrance parameters/% @ 263 K; 200 K; 183 K	98.7; 70; 60
$\langle\Delta E_{all}\rangle_{N_2}$/kcal mol^{-1} @ 263 K; 200 K; 183 K	2; 8; Very High $\beta = 1$
(b) ClOClO and ClO–ClO	
ClOClO	
Critical energy at 0 K/kcal $mole^{-1}$	9.45
Frequencies/cm^{-1}	1015, 622, 441, 354, 258, 116
Product of adiabatic moments of inertia/AMU-A^2	230.4
Moment of inertia: Active external rotor/AMU-A^2	29.5
ClO–ClO (Transition state)	
Frequencies/cm^{-1}	866, 866
Anharmonicities/cm^{-1}	7.5, 7.5
Active external rotor/AMU-A^2 (K-rotor)	29.5
Mean of adiabatic moments of inertia/AMU-A^2 (J-rotor) 263 K; 200 K; 183 K	1243; 1325; 1351
Hindrance parameters/% @ 263 K; 200 K; 183 K	98.7; 70; 60
$\langle\Delta E_{all}\rangle_{N_2}$/kcal mol^{-1} @ 263 K; 200 K; 183 K	2; 8; Very High $\beta = 1$

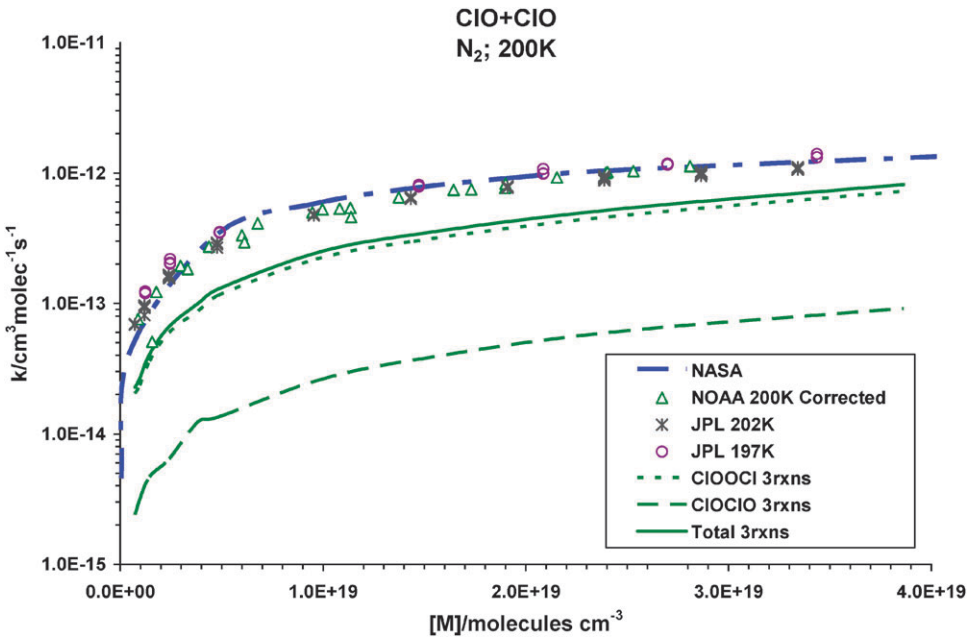

Fig. 4 The blue curve is from the NASA/JPL[4] compilation, the data are referenced therein; the green curves are for ClOOCl, ClOClO formation and their sum.

the results quantitatively and their results have been the basis for the values in the NASA/JPL4 evaluation. Two different studies have presented potential energy surfaces for this system[29,30] and this offered an opportunity to revisit the experiments employing MultiWell.[11,12] Both of these studies are in good agreement with respect to the structure, frequencies and heats of formation of the stable species. They are also in agreement on the structure, frequencies and heat of formation of the transition state for *cis-trans* isomerization in ClONO. They differ substantially on the transition states for chlorine atom association with nitrogen dioxide to form *cis* and *trans* ClONO and $ClNO_2$.

RRKM/master equation analysis

Since the data appear to be at or very close to the low-pressure limit, the full RRKM/ME analysis will not be very sensitive to the detailed nature of the transition state. However, since the transition states are located at of near the centrifugal barriers and these affect the energy available for the reaction, the usual procedure for taking this into account is outlined below. Also, it is of interest to confirm that the data in the measured regions are indeed in the low-pressure limit.

The analysis proceeded in the following fashion:

1. Structure and frequencies for *cis*- and *trans*-ClONO and $ClNO_2$ were taken from the literature.

2. Using the Cartesian coordinates from the above structures, the values of the internuclear distance at the centrifugal maxima were computed. There are several ways to compute the moments of inertia at the transition state.

(a) One method for the "loose" transition states, has been presented several times already in this Review. Using a Morse potential, computed using the center of mass coordinate, the position of the centrifugal maximum was obtained by adding the rotational energy at the maximum and setting the derivative to zero. The Morse β parameter can be computed from the appropriate frequency and bond energy: $\beta = 2\pi c\omega(\mu/De)^{1/2}$ or from force constants: $\beta = (f/2De)^{1/2}$. Using this method, values for the ratio of moments in the transition state (or activated species) $I^{\neq}/I$ are 5.79 ($ClNO_2$) and 3.65 (ClONO) at 300 K.

(b) Another method, which has been adopted here, uses formulae due to Troe[31] to compute the effective ratio of moments at the transition state to that of the stable molecule. These formulae require the calculation of the maxima as a function of the J quantum number, the centrifugal barriers. The formulae differ for linear and nonlinear species. Using the value for linear species, which applies here because the rotation around the figure axis, the "K-rotor" has been included in the density of states in the MultiWell calculation, values for the ratio of moments in the transition state (or activated species) $I^{\neq}/I$ are 5.38 ($ClNO_2$) and 3.43 (ClONO) at 300 K, almost identical to those above.

3. Frequencies and moments of inertia for the Gorin rotors in the transition state were those of NO_2 used previously.[19] The low-pressure limit and pressures close to this limit, are not particularly sensitive to these values.

4. Energy transfer with the nitrogen bath gas was computed using the exponential down probability function and the value of $\langle \Delta E_d \rangle$ could be adjusted in an attempt to reproduce experiment. In fact, there are sufficient uncertainties in so many input parameters that only computations using 500 cm^{-1} as the value of $\langle \Delta E_d \rangle$ are reported.

5. Since all the data are in, or very close to, the low-pressure limit, the NASA/JPL[4] values for the high pressure limit are little more than estimates. Hindrance values of 0% (Full Gorin model) were chosen as a starting point and there is little reason to get more detailed. The equilibrium constant was calculated from the appropriate values of the enthalpy and the structure and frequencies of *cis* and *trans* ClONO and $ClNO_2$, Cl and NO_2 using the "Thermo" code in MultiWell.[11,12]

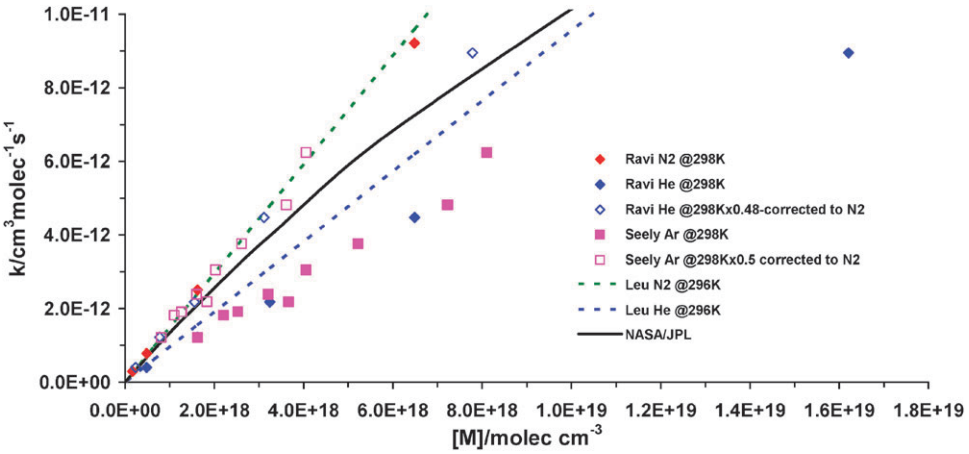

Fig. 5 Data at 298 K and the value from the NASA/JPL Evaluation.[4] Measured data are depicted with solid symbols. Open symbols are corrected to N_2 as the bath gas.

The "hindered-Gorin" transition state. Not much restriction is to be expected when one of the reactants is an atom. So transition states for the barrierless association reactions were generated as discussed several times in this Review. Using the hindered-Gorin model, values for the high pressure limit rate constant for $ClNO_2$ and ClONO forming pathways turns out to be about 8×10^{-11} and 1×10^{-10} cm^3 $molecules^{-1}$ sec^{-1}, respectively.

Energy transfer parameters. The initial value chosen for $\langle \Delta E_d \rangle$ was 300 cm^{-1}. This seemed "reasonable" based on experience, but represents a fitting parameter which can make up for a gap in knowledge that includes the probability distribution function for energy transfer, the actual value, or values, of the energy transferred in a collision, as well as the lack of consideration of anharmonicity and the possibility that the two-dimensional rotors should not be taken as adiabatic. A somewhat high value of 500 cm^{-1} was finally chosen. ($\langle \Delta E_d \rangle$ can be temperature dependent, this kind of variation was not employed here. It is entirely conceivable that small changes in some of the other fitting parameters would accommodate a temperature dependence for $\langle \Delta E_d \rangle$.)

Fig. 5 shows most of this data. Some caveats: The data labeled "Leu" were only taken at pressures up to 10 torr (3×10^{17}), the lines are extrapolations of the reported 3rd order rate constants. The data labeled "Ravi He@298K-corrected to N_2" were plotted by multiplying the He pressures by 0.48 to bring them into agreement with the N_2 data. Although the "Leu N_2@296K" data and "Ravi N_2@298K" are in agreement, the corresponding He data differ by about 35%. The correction to the "Seely Ar@298K" data was done by multiplying the Ar pressures by 0.5 to bring the lowest points into agreement with the "Ravi N_2@298K". Experience with other systems suggests that this factor of two difference between Ar and N_2 may be somewhat too great. So there is a modicum of uncertainty to the data. The NASA Sum line is the result from the NASA/JPL evaluation[4] for the sum of values for the formation of ClONO (*cis* and *trans* were not differentiated) and $ClNO_2$. This latter curve implies that the data at the higher pressures show the effect of pressure fall-off.

Values of the rate constants are underpredicted in the low pressure regime. Although experiment[32] seems to suggest that the ClONO species should be formed at 3 to 4 times the rate for $ClNO_2$, the results from the Gorin calculations do not show this. As a way of enhancing the ratio of ClONO to $ClNO_2$ formation, the stability of the ClONO isomers was enhanced by 2 kcal mol^{-1}, which would seem to be within the uncertainty in the calculated stabilities. The value of $\langle \Delta E_d \rangle$ used was 500 cm^{-1}. The results, which still underpredict the data, are shown as the red lines in comparison to the data in Fig. 6.

Once again, it is found that the underprediction of the data can be alleviated by some arbitrary, changes in parameters or constraints. Thus if the Lennard-Jones collision parameters are increased and/or the two dimensional rotors are taken as active, the data can be accommodated. Also, anharmonicity corrections to the density of states may solve the problem.

$ClNO_2$ decomposition

There are some studies of the thermal decomposition of $ClNO_2$ in Ar between 678 and 1032 K at molecular densities ranging from 7.5×10^{18} at the lowest temperature to 4.2×10^{18} molecules cm^{-3} at the highest and in pure $ClNO_2$ at temperatures between 453 K and 521 K. Second order rate constants were studied directly. Also experiments in Ar at only 453 K with molecular densities in the range 1.2×10^{17} to 1.5×10^{18} molecules cm^{-3} were reported. A second order rate constant was extracted from the data at densities up to about 3×10^{17}.

Calculations using the parameters that produced the pink lines in Fig. 6, yield values that result in slightly higher values than the higher temperature data, so if these data are taken at face value and the parameters for $ClNO_2$ are adjusted to comply, computations of the type shown in Fig. 6 would be further from the data shown in that figure. On the other hand, the lower temperature data is higher than the calculation in keeping with the observation at 300 K. There is a message here about consistency among experimental studies.

An observation, which is consistent with other studies in this Review, is that the most uncertain part of knowledge for

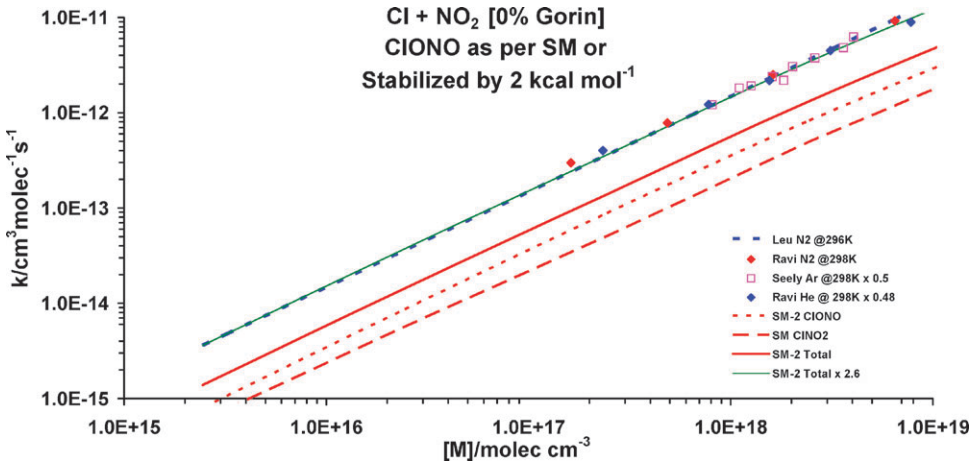

Fig. 6 Data as in Fig. 5. The pressure range is where data exist. Red curves are computed with both isomers of ClONO and the isomerization transition state stabilized by 2 kcal mol^{-1}. $\langle \Delta E_d \rangle$ = 500 cm^{-1} for all curves in this figure. The $ClNO_2$ curve is unaffected by the change in stability of ClONO. The green line is the solid red line multiplied arbitrarily by 2.6 to fit the data.

pressure dependent unimolecular and association reactions is in the low pressure limit. Effects due to: accurate values of heats of formation, probability distribution and amounts of energy transferred, the interaction of rotation and vibration, and anharmonicity all play a role. Note should also be taken of the fact that the data are not without some uncertainty. So for reactions close to the low-pressure limit, extrapolation out of the experimental range would seem to be subject to large uncertainties.

IO + NO_2 ↔ $IONO_2$

Data for this system have been analyzed[33] *and references are found in that work*. It was found that once again the low pressure end of the pressure curves was underpredicted. In this study it was shown that increasing the, then uncertain, bond dissociation energy to *ca*. 150 kJ $mole^{-1}$ increased the state density sufficiently to match the data. Since that study, there have been several attempts to discern a reliable bond dissociation energy for $IONO_2$. From a Private Communication from Paul Marshall, relevant values are: $\Delta H_{f,298}(HOI) = -59.2 \pm 3.3$ kJ/mol; $\Delta H_{f,298}$ ($IONO_2$) = 37.4 ± 3.9 kJ/mol; $\Delta H_{f,0}$($IONO_2$) = 45.8 ± 3.9 kJ/mol. Using $\Delta H_{f,0}(IO) = 122.6 \pm 2.4$ kJ/mol the value for the bond dissociation energy at 0 K, $\Delta H_{f,0}(IO) + \Delta H_{f,0}(NO_2) - \Delta H_{f,0}(IONO_2) = 113.6 \pm 3.1$ kJ/mol. Thus another reason for the underprediction will need to be discerned. The culprits, once again are likely to be, anharmonicity, understanding of collisional energy transfer and possibly the inclusion of the two dimensional rotations as active.

BrO + NO_2 ↔ $BrONO_2$

This section summarizes a study by Walsh and Golden.[34] *References are found in that work*. Experimental data for the title reaction have been modeled using Master equation/RRKM methods based on the MultiWell suite of programs. The starting point for the exercise, as before, was the empirical fitting provided by the NASA[4] and IUPAC[3] data evaluation panels, which represent the data in the experimental pressure ranges rather well. Despite the availability of quite reliable parameters for these calculations (molecular vibrational frequencies and a value of $D_{298}(BrO–NO_2)$ = 118 kJ mol^{-1}, corresponding to ΔH_0^0 = 114.3 kJ mol^{-1} at 0 K.) once again, there is a discrepancy between the calculations and the data base of rate constants of a factor of *ca* 4 at, or close to, the low-pressure limit. Fitting, or close, could be achieved in several ways, either by increasing $\Delta H_0^0$to 149.3 kJ mol^{-1}, or by increasing $\langle \Delta E_d \rangle$, the average energy transferred in a downward collision, to unusually large values. Since the bond energy seems to be supported by experiment and theory, only the latter or the incorporation of the two dimensional rotations into the state density, are left. Of course, it is possible, even probable, that anharmonicity factors, including all off diagonal terms, may increase the density of states sufficiently to explain the data. The system was relatively insensitive to changing the moments of inertia in the transition state to increase the centrifugal effect. The possibility of involvement of BrOONO was tested and cannot account for the difficulties of fitting the data.

RRKM/Master equation analysis

As in earlier examples, the analysis proceeded in the following fashion:

1. The structure and frequencies for $BrONO_2$ were taken from the literature.

2. As delineated earlier, using the aforementioned geometries, the moments of inertia of $BrONO_2$ and BrOONO were computed. The two-dimensional (2D) moment of inertia is the root mean square of the two largest moments (J moment). Using a Morse potential, and the known well depth, the position of the centrifugal maximum was obtained by adding the rotational energy at the maximum. These values were then used to replace the $BrO–NO_2$ and BrO–ONO equilibrium bond lengths and moments of inertia were calculated for these new entities, *viz*. the transition states. This was done at each temperature of interest, but in the limited temperature range of the data, 251 K to 346 K, the values change very little.

3. Frequencies and moments of inertia for the transition states were taken to be those of NO_2, used previously,[19] and BrO, from the JANAF Tables.[35] The structure and frequencies

for the transition state for isomerization between the nitrate and peroxynitrous forms were estimated.

4. Energy transfer with the nitrogen bath gas was computed using the exponential down probability function and the value of $\langle \Delta E_d \rangle$, the average energy transferred in a downward step, was set at 400 cm^{-1}, which as suggested previously is a reasonable value for N_2.[33] Normal uncertainties in this and the other collision parameters do affect the fitting of the calculated curves to the results, but often the data can be accommodated with only small changes in these quantities. As will become apparent below, the only way that data could be fit for this BrO + NO_2 system was to make enormous changes in $\langle \Delta E_d \rangle$.

5. If the energy transfer parameter is taken to be given from experience as the normal value above, the key variables which determine the extent of rate constant pressure dependence are the degree of hindrance (which determines the high pressure limiting *A* factor) and the critical energy (which determines the low-pressure limiting rate constant). The choice of these is discussed in the next sections.

6. As usual, it is necessary to know the equilibrium constants in order to compute the association rate constants. The equilibrium constants were calculated using the "Thermo" code within MultiWell, which employs the same input information as for the RRKM calculation itself.

The "hindered-Gorin" transition state

Degrees of hindrance for the transition states were chosen to match the high pressure rate constants obtained by the NASA formula. The critical energy ΔE_0^0 used corresponds to ΔH_0^0 = 114.3 kJ mol^{-1}, use of the theoretical value[9] of 121.8 kJ mol^{-1} made only small differences.

Calculations and results

Two-well MultiWell calculations were performed using the parameters in Table 4. Note that the two dimensional rotations of $BrONO_2$ and BrO–NO_2 are assumed to be adiabatic. The wells correspond to $BrONO_2$ and BrOONO. Each may be formed from interaction of BrO and NO_2. In addition they may interconvert over a small barrier *via* a cyclic transition state that has been estimated in this study. Two calculations can be made for each temperature. One starting with a chemical activation energy distribution for $BrONO_2$ formed from BrO and NO_2 and one starting with a chemical activation energy distribution for BrOONO formed from these species. (In fact only small contributions at high pressures arise from the pathway through chemically activated BrOONO*.) Computations were performed in attempts at fitting the NASA/JPL curve, but except for different hindrance values to fit the high pressure region, the discussion covers the IUPAC evaluation as well, since the data are all in the low pressure region and both evaluations fit the data.

A first approximation assumed that the high pressure rate constants for each path were equal and the hindrances were chosen to reflect that assumption. Fig. 7 shows the data, the NASA evaluation and the results of the two-well fit in the pressure range corresponding to the data. The red line labeled

Table 4 Parameters for MultiWell calculations for $BrONO_2$ dissociation

$BrONO_2$ (Molecule)	
Critical energy at 0 K/kJ mol^{-1}	114.3
Vibrational wavenumbers/cm^{-1}	1743, 1321, 818, 747, 744, 560, 393, 209
Hindered internal rotor:wavenumber/cm^{-1}; Moment of inertia/amu A^2; Rotational symmetry	112; 12.56; 2
(J-rotor) Adiabatic moments of inertia /amu A^2	315.7
(K-rotor) Active external rotor/amu A^2	41.5
Symmetry; Degeneracy; Optical isomers	1; 1; 1
BrO–NO_2 (Transition state)	
Vibrational wavenumbers/cm^{-1}	1618, 1318, 750, 727
(J-rotor) Adiabatic moments of inertia/amu A^2	675.7 (251 K); 671.7 (268 K); 664.8 (300 K); 656.0 (346 K)
(K-rotor) Active external rotor/amu A^2	56.8 (251 K); 56.8 (268 K); 56.6 (300 K); 56.4 (346 K)
Moments of inertia active 2-D rotors/amu A^2	39.3 (BrO); 9.34 (NO_2)
Hindrances(%)	83.7 (251 K); 86.9 (268 K); 91.0 (300 K); 94.3 (346 K)
Symmetry; Degeneracy; Optical isomers	1; 1; 1
LJ collision parameters: (σ/A^2; ε/K;)	5.2; 450 ($BrONO_2$), 3.74; 82 (N_2)
$\langle \Delta E \rangle_{down}$/$cm^{-1}$	See Text
BrOONO (Molecule)	
Critical energy at 0 K/kJ mol^{-1}	20.2
Vibrational wavenumbers/cm^{-1}	1846, 980, 676, 560, 443, 307, 265
Hindered internal rotors:wavenumber/cm^{-1}; Moment of inertia/amu A^2; Rotational symmetry	210, 4.22, 1 125, 42.8, 1
(J-rotor) Adiabatic moments of inertia/amu A^2	312.4
(K-rotor) Active external rotor/amu A^2	61.0
Symmetry; Degeneracy; Optical isomers	1; 1; 2
BrO–ONO (Transition state) 300 K Only	
Vibrational wavenumbers/cm^{-1}	1618, 1318, 750, 727
(J-rotor) Adiabatic moments of inertia/amu A^2	805.9
(K-rotor) Active external rotor/amu A^2	2.19
Moments of inertia active 2-D rotors/ amu A^2	39.3 (BrO); 9.34 (NO_2)
Hindrance (%)	94.5
Symmetry; Degeneracy; Optical isomers	1; 1; 1
LJ collision parameters: (σ/A^2; ε/K;)	5.2; 450 (BrOONO), 3.74; 82 (N_2)
$\langle \Delta E \rangle_{down}$/$cm^{-1}$	See Text

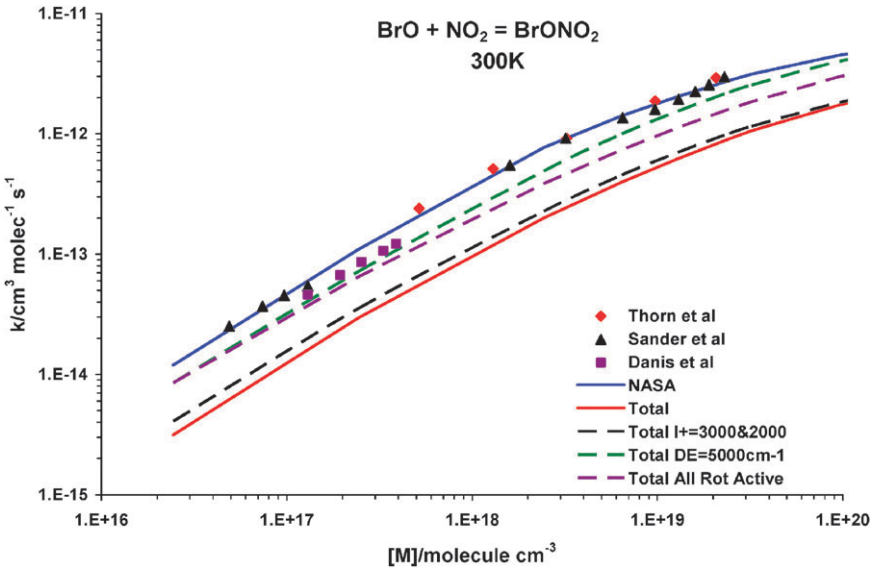

Fig. 7 Comparison of data,[4] empirical fits and modeling for the title reaction at 300 K. The solid red line marked "Total" is for the total loss of reactants in the standard two well ($BrONO_2$ and BrOONO) computation using parameters from Table 3. The dashed black line marked "Total I + = 3000&2000" represents the effect of increasing the moments of inertia of the transition states leading to $BrONO_2$ and BrOONO to 3000 and 2000 AMU-A^2, respectively. The dashed green line marked "Total DE = 5000 cm^{-1}" represents the results when the value of $\langle \Delta E_d \rangle$ is increased to 5000 cm^{-1}. The dashed violet line represents the results when all rotations are taken as active.

"Total" shows the formation *via* both pathways. The pathway *via* chemically activated BrOONO only contributes at the highest pressures in the calculation, which are well above the experimental range. Most notable is the lack of fitting the data at low pressures, where the data are some four times higher than the calculations. The black dashed line labeled "Total I + = 3000&2000" was computed with the very unphysical assumption that the moments of inertia of the transition states for and BrOONO were respectively increased to 3000 and 2000 AMU-A^2, respectively. This shows that the difference between experiment and calculation is not due to errors in these moments. Three possibilities come to mind, the critical energy must be much higher than thought, or the energy transfer must be much more efficient than expected, or finally all rotations are active. In fact, the data can be fit by raising the bond energy to a value in the neighborhood of 150 kJ mol^{-1}, however, given the earlier discussion of the bond energy, it would seem that only small variations are possible and this value is out of the range. Thus, to see what else could be changed to fit the data, the value of $\langle \Delta E_d \rangle$ was raised to the seemingly unphysical value of 5000 cm^{-1}. This comes close (within 50% at the low pressures) to fitting the data as can be seen from the green dashed line in Fig. 7. (Lowering the isomerization barrier from 14.6 to 4.2 kJ mol^{-1} raised the rate constants by about 10%.) Presumably larger values for $\langle \Delta E_d \rangle$ will fit even better, but they do seem unrealistic. In Fig. 7 the violet dashed line, also illustrates that the data are similarly matched by assuming all rotations to be active, but this cannot be increased further.

Calculations at the other reported temperatures show similar discrepancies with the data. It seems clear that arbitrarily raising $\langle \Delta E_d \rangle$ will also accommodate those data. The dissociation data[4] are similarly underpredicted.

Discussion

The methods described in this Review have been applied to several systems. Interestingly, results of such calculations are in reasonable concert with the data for CH_4 dissociation along with CH_3 + H association,[17] reactions[19] of OH with NO_2 and for what would seem to be disparate systems such as CH_3 decomposition and the dissociation and reverse of CH_3O_2-NO_2. However, problems exist for the association[33] of IO with NO_2 and[27] Cl with NO_2 and[34] BrO with NO_2. It seems clear that the value of the high pressure limiting rate constants, including temperature dependence, can be characterized with the hindered-Gorin approach. The hindrance values are purely empirical, but as potential energy surfaces are developed for the systems of practical interest being studied, it should be possible to approach theoretical values for this quantity.

On the other hand, the low pressure limit presents a more difficult problem in some cases. The methods employed here involve the use of a one dimensional master equation, since calculations seem to be relatively insensitive to rational values of $I^{\neq}$, it isn't clear that a two dimensional calculation will improve the situation much. Setting all the rotational energy as active often falls short of matching the data and is not required in those cases where the methodology seems adequate. Understanding of the energy transfer process, although heavily studied, is not well understood. In all the calculations, the exponential down probability distribution has been employed. There are others, the MultiWell suite offers several. Perhaps different systems would be better described with different choices for this function. Or, perhaps those systems containing halogen atoms really do transfer energy with large step sizes. As alluded to earlier, it is possible that anharmonicity effects that include all off diagonal terms, may increase the density of states sufficiently to cover the discrepancy and

maybe this is more important in those systems containing halogen atoms.

Summary

There is significant uncertainty in the theory of unimolecular reactions, particularly with respect to energy transfer and there are difficulties in obtaining various physical parameters derived from the poorly described potential energy surfaces that often obtain. Assuring reasonable agreement with theory is satisfying, but spending much time and energy on details needed to represent pressure dependent rate coefficients for use in atmospheric, combustion, or other models of "engineering" problems does not seem terribly worthwhile. For processes to which the model is very sensitive, experimental values would be best. Otherwise using the best values available and systematically optimizing within reasonable error bounds is recommended.

Acknowledgements

The author acknowledges support through Grant # NNG06GF98G "Critical Evaluation of Kinetic Data/Applied Theory" from The NASA Upper Atmosphere Research Program and by Grant CHE-0535555 from The National Science Foundation "Process Informatics for Chemical Reaction Systems".

Collaboration with John R. Barker and Robin Walsh is acknowledged as well.

Also, the author is very pleased to participate in honoring the career of his friend of over four decades Professor Robin Walsh!

References

1 R. Feeley, M. Y. Frenklach, M. Onsum, T. Russi, A. Arkin and A. Packard, *J. Phys. Chem. A*, 2006, **110**, 6803.
2 M. Y. Frenklach, A. Packard, P. Seiler and R. Feeley, *Int. J. Chem. Kinet.*, 2004, **36**, 57.
3 R. Atkinson, D. L. Baulch, R. A. Cox, J. R. F. Hampson, J. A. Kerr, M. J. Rossi and J. Troe, *J. Phys. Chem. Ref. Data*, 2000, **29**, 167.
4 S. P. Sander, B. J. Finlayson-Pitts, R. R. Friedl, D. M. Golden, R. E. Huie, C. E. Kolb, M. J. Kurylo, M. J. Molina, G. K. Moortgat, V. L. Orkin and A. R. Ravishankara, *'Chemical Kinetics and Photochemical Data for Use in Atmospheric Studies, Evaluation Number 15'*, JPL Publication 02-25, Jet Propulsion Laboratory, Pasadena, 2006.
5 D. L. Baulch, C. T. Bowman, C. J. Cobos, R. A. Cox, T. Just, J. A. Kerr, M. J. Pilling, D. Stocker, J. Troe, W. Tsang, R. W. Walker and J. Warnatz, *J. Phys. Chem. Ref. Data*, 2005, **34**, 757.
6 J. R. Barker and D. M. Golden, *Chem. Rev.*, 2003, **103**, 4577.
7 G. P. Smith, D. M. Golden, M. Frenklach, N. W. Moriarty, B. Eiteneer, M. Goldenberg, C. T. Bowman, R. K. Hanson, S. Song, W. C. Gardiner, Jr, V. V. Lissianski and Z. Qin, in *'GRI-Mech 3.0'*, http://www.me.berkeley.edu/gri_mech/, 2000.
8 M. Y. Frenklach, *Proc. Combust. Inst.*, 2007, **31**, 125.
9 J. A. Miller and S. J. Klippenstein, *J. Phys. Chem. A*, 2006, **110**, 10528.
10 S. H. Robertson, M. J. Pilling, L. C. Jitariu and I. H. Hillier, *Phys. Chem. Chem. Phys.*, 2007, **9**, 4085.
11 J. R. Barker, *Int. J. Chem. Kinet.*, 2001, **33**, 232.
12 J. R. Barker, in '*MultiWell-2.01 Software, APR 2006, designed and maintained by J. R. Barker with contributions from N. F. Ortiz, J. M. Preses, L. L. Lohr, A. Maranzana, and P. J. Stimac; University of Michigan, Ann Arbor, MI*; http://aoss.engin.umich.edu/multiwell/.', 2006.
13 S. E. Stein and B. S. Rabinovitch, *J. Chem. Phys.*, 1973, **58**, 2438.
14 K. A. Holbrook, M. J. Pilling and S. H. Robertson, *'Unimolecular Reactions'*, Wiley, 1996.
15 J. A. Miller, S. J. Klippenstein and C. J. Raffy, *J. Phys. Chem. A*, 2002, **106**, 4904.
16 D. M. Golden, *Int. J. Chem. Kinet.*, 2005, **37**, 625.
17 D. M. Golden, *Int. J. Chem. Kinet.*, 2007, in press.
18 P. H. Stewart, G. P. Smith and D. M. Golden, *Int. J. Chem. Kinet.*, 1989, **21**, 923.
19 D. M. Golden, J. R. Barker and L. L. Lohr, *J. Phys. Chem. A*, 2003, **107**, 11057.
20 H. Hippler, N. Krasteva, S. Nasterlack and F. Striebel, *J. Phys. Chem. A*, 2006, **110**, 6781.
21 J. Zhang and N. M. Donahue, *J. Phys. Chem. A*, 2006, **110**, 6898.
22 W. I. Spartan '02, Irvine, CA.
23 V. Vasudevan, R. K. Hanson, D. M. Golden and C. T. Bowman, *J. Phys. Chem. A*, 2007, **111**, 4062.
24 D. M. Golden, *Int. J. Chem. Kinet.*, 2003, **35**, 206.
25 J. Plenge, S. Kuhl, B. Vogel, R. Muller, F. Stroh, M. von Hobe, R. Flesch and E. Ruhl, *J. Phys. Chem. A*, 2005, **109**, 6730.
26 J. Liu and J. R. Barker, *J. Phys. Chem. A*, 2007, **111**, 8689.
27 D. M. Golden, *J. Phys. Chem. A*, 2007, **111**, 6772.
28 J. S. Chang, A. C. Baldwin and D. M. Golden, *J. Chem. Phys.*, 1979, **71**, 2021.
29 H. Sayin and M. L. McKee, *J. Phys. Chem. A*, 2005, **109**, 4736.
30 R. S. Zhu and M. C. Lin, *ChemPhysChem*, 2004, **5**, 1864.
31 J. Troe, *Chem. Rev.*, 2003, **103**, 4565.
32 H. Niki, P. D. Maker, C. M. Savage and L. P. Breitenbach, *Chem. Phys. Lett.*, 1978, **59**, 78.
33 D. M. Golden, *J. Phys. Chem. A*, 2006, **110**, 2940.
34 R. Walsh and D. M. Golden, *J. Phys. Chem. A*, 2008, **112**, submitted.
35 M. Chase, Jr, *J. Phys. Chem. Ref. Data*, 1998, Monograph No. 9, 1404.